Acta Cryst E CRYSTALLOGRAPHIC COMMUNICATIONS

ISSN 2056-9890

Synthesis and structure of 2-amino-4-methylpyridin-1-ium hippurate dihydrate

Vanitha Vetrivel,[a] Nishandhini Marimuthu[b]* and Thangavelu Balakrishnan[a]*

[a]Crystal Growth Laboratory, PG and Research department of Physics, Thanthai Periyar Government Arts and, Science College (Autonomous), affiliated to Bharathidasan University, Tiruchirappalli, Tiruchirappalli-620 023, Tamil Nadu, India, and [b]Department of Bioinformatics, VISTAS, Chennai, Tamil Nadu, India. *Correspondence e-mail: bionisha@gmail.com, balacrystalgrowth@gmail.com

Received 6 April 2026
Accepted 10 May 2026

Edited by W. T. A. Harrison, University of Aberdeen, United Kingdom

Keywords: crystal structure; 2-amino-4-methylpyridin-1-ium cation; hippurate anion; Hirshfeld surface analysis.

CCDC reference: 2552915

Supporting information: this article has supporting information at journals.iucr.org/e

In the extended structure of the title salt, $C_6H_9N_2^+\cdot C_9H_8NO_3^-\cdot 2H_2O$, the 2-amino-4-methylpyridin-1-ium cation and hippurate [or 2-(phenylformamido)-acetate] anion are linked through paired N—H···O hydrogen bonds, forming an $R_2^2(8)$ motif. The water molecules of crystallization participate in O—H···O and N—H···O hydrogen-bonding interactions, which connect the molecular components into one-dimensional chains that extend along the [010] direction. These interactions collectively generate a three-dimensional supramolecular network.

1. Chemical context

Pyridinium-based organic salts continue to attract interest owing to their diverse supramolecular architectures and their ability to form robust hydrogen-bonded networks in the solid state (Konovalova & Reiss, 2025; Bis & Zaworotko, 2005; Budzikur *et al.*, 2022). 2-Amino-4-methylpyridine, $C_6H_8N_2$, is a bi-functional heterocycle containing both a basic pyridine nitrogen (ring N atom) and an exocyclic amino group (-NH_2), enabling different hydrogen-bonding patterns and facilitating salt formation with a variety of organic acids. Protonated aminopyridines are widely used as structure-directing cations because their multiple donor and acceptor sites support extended N—H···O, O—H···O, and π-associated supramolecular motifs in the solid-state (Bedeković *et al.*, 2017; Desiraju, 2002; Aakeröy & Seddon, 1993).

Hippuric acid (benzoylglycine, $C_9H_9NO_3$) is a biologically relevant carboxylic acid that mimics short peptide fragments and provides several potential donor/acceptor sites through its carboxyl, amide, and aromatic groups (Li *et al.*, 2024). Both hippuric acid and its deprotonated hippurate (benzoylglycinate, $C_9H_8NO_3^-$) anions are widely employed in organic salts and co-crystals, where their amide, carboxylate, and aromatic functionalities enable complementary hydrogen-bonding interactions and π-stacking contacts (Laishram *et al.*, 2025; Suganya *et al.*, 2021).

Proton transfer in crystalline acid–base systems is commonly rationalized using the ΔpK_a rule (Cruz-Cabeza, 2012, 2022): when the difference between the pK_a of the conjugate acid of the base and the pK_a of the acid exceeds $\simeq$ 2–3, salt formation is favored. For the present system, the reported pK_a values (hippuric acid $\simeq$ 3.6 and 2-amino-4-methylpyridinium ion $\simeq$ 7.5–8.1) gives $\Delta pK_a \simeq 3.9$, supporting proton transfer and the formation of a 2-amino-4-methylpyridinium benzoylglycinate salt. Such a proton transfer leads to the formation of charge-assisted N^+—H···O hydrogen

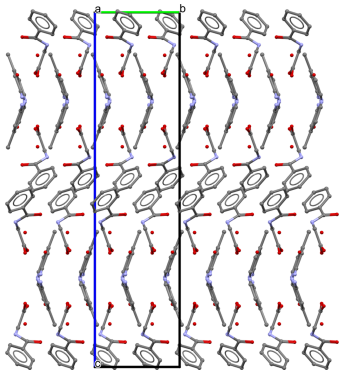

bonds, which are typically shorter, and more electrostatically strengthened than their neutral counterparts; these interactions often dominate the molecular packing, enhance crystal cohesion and facilitate the incorporation of water molecules of crystallization that further connect the ions through O—H···O and O—H···N hydrogen bonding.

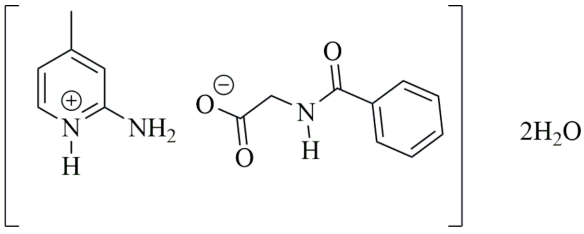

As part of our studies in this area, we now describe the synthesis, structure and Hirshfeld surface analysis of the title hydrated salt, $C_6H_9N_2^+\cdot C_9H_8NO_3^-\cdot 2H_2O$ (**I**).

2. Structural commentary

The hydrated title salt (**I**) was obtained by proton transfer from hippuric acid to 2-amino-4-methylpyridine in aqueous solution. The crystal structure unambiguously confirms salt formation through a proton-transfer reaction, which is consistent with the acidity constants of the components noted above, which strongly favors salt formation rather than co-crystallization

Compound (**I**) crystallizes as orthorhombic in space group *Pbca*. The asymmetric unit consists of one 2-amino-4-methylpyridin-1-ium cation, one hippurate anion and two water molecules of crystallization, as illustrated in Fig. 1. In the cation, proton migration to the pyridine nitrogen atom (N2) is further supported by the increase in the internal angle around the protonated nitrogen atom [C10—N2—C14 = 122.22 (13)°], compared with 117.3 (1)° in neutral 2-amino-4-methylpyridine (Kvick & Noordik, 1977). The bond lengths and angles of the cation closely resemble those observed in related structures, including 2-amino-4-methylpyridin-1-ium hydrogen squarate (Vetrivel *et al.*, 2025) and other similar protonated analogues (Khalib *et al.*, 2014). The non-hydrogen atoms of the cation are essentially planar, with a maximum deviation of 0.027 (3) Å for atom C15. In the hippurate anion,

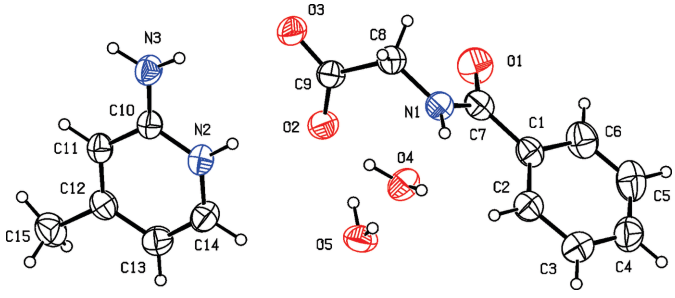

Figure 1
The molecular structure of the title salt, (**I**), showing the atom-labelling scheme. Displacement ellipsoids are drawn at the 50% probability level.

Table 1
Hydrogen-bond geometry (Å, °).

D—H···A	D—H	H···A	D···A	D—H···A
O5—H5A···O4	0.83 (2)	2.00 (2)	2.8225 (18)	167 (3)
N1—H1···O4^{i}	0.85 (1)	2.25 (2)	2.9992 (18)	148 (2)
N2—H2A···O3^{ii}	0.90 (2)	1.78 (2)	2.6850 (17)	176 (2)
N3—H3A···O2^{ii}	0.89 (2)	1.99 (2)	2.8751 (17)	175 (2)
N3—H3B···O5^{iii}	0.90 (2)	1.94 (2)	2.8368 (18)	171 (2)
O4—H4A···O3^{iv}	0.88 (2)	1.88 (2)	2.7392 (17)	166 (2)
O4—H4B···O1^{v}	0.87 (2)	1.95 (2)	2.8173 (18)	173 (2)
O5—H5B···O2^{i}	0.88 (2)	1.94 (2)	2.8061 (18)	170 (3)

Symmetry codes: (i) $-x+1, -y+1, -z+1$; (ii) $-x+\frac{1}{2}, -y+1, z-\frac{1}{2}$; (iii) $-x+\frac{1}{2}, y-\frac{1}{2}, z$; (iv) $x+\frac{1}{2}, -y+\frac{3}{2}, -z+1$; (v) $-x+1, -y+2, -z+1$.

the carboxylate group has nearly equivalent C—O bond lengths [O2—C9 = 1.2377 (18) Å and O3—C9 = 1.2598 (19) Å; Δ = 0.0221 Å], confirming deprotonation (Table 1). The key torsion angles for the side chain are C1—C7—N1—C8 = −175.96 (12)° and C7—N1—C8—C9 = −87.11 (18)° and the dihedral angle between the C1–C6 phenyl ring and the carboxylate plane (O1/O2/C8/C9) is 70.96 (7)°. These geometric parameters are comparable to those reported for deprotonated hippurate anions in related crystal structures, such as cytosinium *N*-benzoylglycinate monohydrate (Görbitz & Sagstuen, 2004).

3. Supramolecular features

In the extended structure, the cation and anion are connected through N2—H2A···O3 and N3—H3A···O2 hydrogen bonds (Table 1, Fig. 2), generating an R_2^2 (8) motif. The two water molecules of crystallization participate actively in the hydrogen-bonding network. In particular, a O5—H5A···O4 hydrogen bond links the two water molecules. All the oxygen atoms of the anion (O1–O3), together with the water O atoms (O4 and O5), function as hydrogen-bond acceptors in various

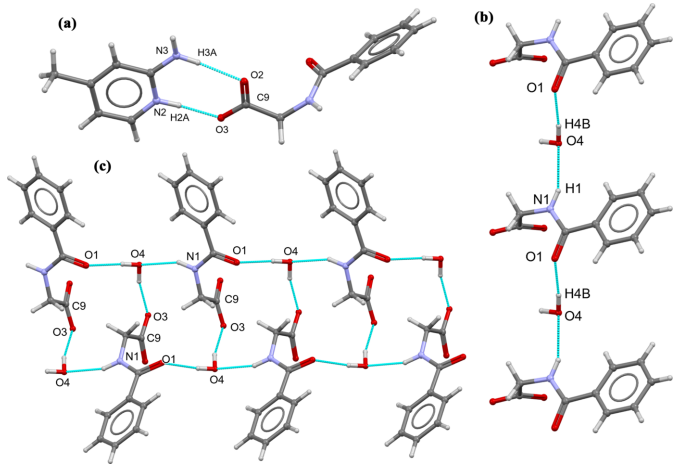

Figure 2
(*a*) Part of the crystal structure of (**I**) showing the $R_2^2(8)$ motif formed by intermolecular N—H···O hydrogen bonds. (*b*) The N1—H1···O4 and O4—H4B···O1 hydrogen bonds connect neighbouring hippurate anions and water molecule O4 (water – 1), forming a one-dimensional chains runs along the [010] direction. (*c*) The O4—H4A···O3, N1—H1···O4 and O4—H4B···O1 hydrogen bonds generate an R_4^4 (16) motif, resulting in a supramolecular ladder-like arrangement running parallel to [010].

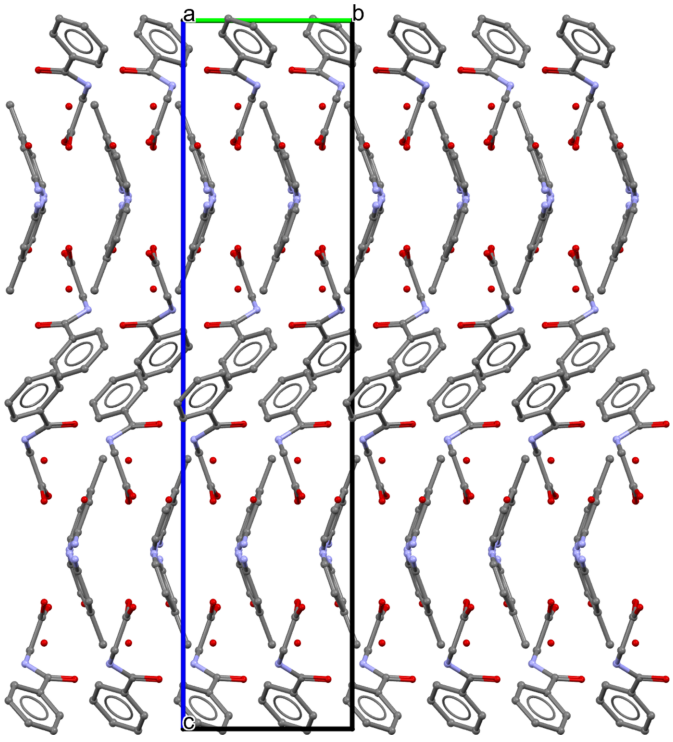

Figure 3
Overall crystal packing of the title salt (**I**), viewed down the *a* axis. Hydrogen atoms have been omitted for clarity.

intermolecular N—H···O and O—H···O interactions (Table 1).

The N1—H1···O4 and O4—H4*B*···O1 hydrogen bonds connect neighbouring hippurate anions and water molecule (water-1, O4), forming four-membered units that propagate into a one dimensional chains extending along the [010] direction. Furthermore, the O4—H4*A*···O3 hydrogen bond along with the N1—H1···O4 and O4—H4*B*···O1 hydrogen bonds, generates an R_4^4 (16) loop, resulting in a supramolecular ladder-like arrangement running parallel to [010]. This ladder is further reinforced by hydrogen bonding involving the cation, namely N2—H2*A*···O3, N3—H3*A*···O2 and O5—H5*B*···O2 and N3—H3*B*···O5, which link the second water molecule (water-2, O5) to the cationic fragment. Collectively, the hydrogen bonds interconnect the cations, anions, and water molecules of crystallization into a three-dimensional supramolecular network (Figs. 3 and 4).

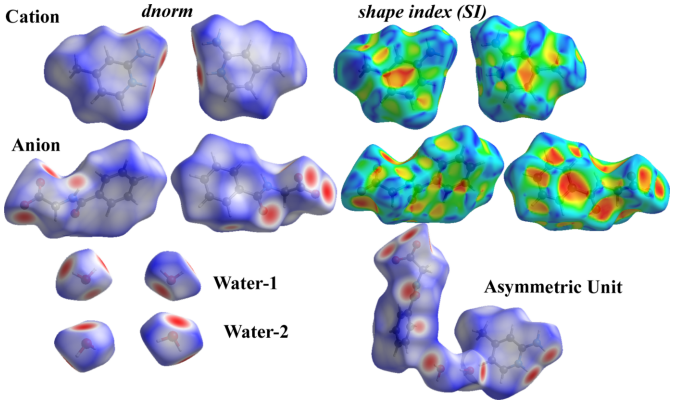

Figure 4
Two views of the Hirshfeld surfaces of the cation, anion and water molecules of crystallization in the title salt (**I**), mapped over d_{norm} and the shape-index surface.

4. Hirshfeld surface analysis

Hirshfeld surface (HS) analysis was carried out using *CrystalExplorer 21.5* (Turner *et al.*, 2017). The front and back views of the HS mapped over d_{norm} for the asymmetric unit are shown in Fig. 4, together with the individual surfaces for the cation, anion and the two water molecules. Bright-red spots on the d_{norm}-mapped surfaces correspond to close contacts, *i.e.*, intermolecular distances shorter than the sum of the van der Waals radii, and thus indicate significant non-covalent interactions. In contrast, the shape-index surface does not exhibit complementary red and blue triangular features, indicating the absence of significant π–π stacking interactions in (**I**).

The full and decomposed two-dimensional fingerprint plots for the cation, anion and the water molecules are presented in Fig. 5. The H···H contacts make the largest contribution for both the cation (50.1%) and the anion (47.1%), and also account for significant contributions in water-1 (40.6%) and water-2 (46.5%). For the water molecules, O···H/H···O contacts are particularly prominent, reflecting their active participation in O—H···O hydrogen bonds. The sharp spikes observed in the FP plots at $d_e + d_i$ = 1.6–1.8 Å for O···H/H···O contacts are characteristic of strong N/O—H···O hydrogen bonds (Table 1). The C···H/H···C interactions represent the next significant contribution in the cation (18.5%) and anion (12.8%). The remaining contacts, namely N···H/H···N, C···N and C···C, contribute comparatively less to the total Hirshfeld surface area. Although both water molecules participate in O—H···O hydrogen bonding, their relative percentage contributions and hydrogen-bond geometries indicate subtle differences in their interaction environments within the crystal.

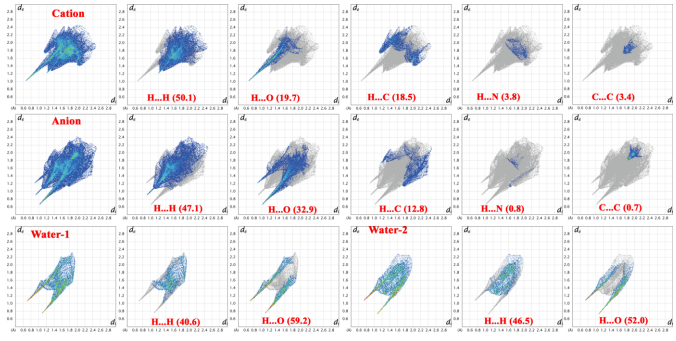

Figure 5
Full and decomposed two-dimensional fingerprint (FP) plots for the cation, anion and the two water molecules of crystallization in the title salt (**I**), showing the different intermolecular contacts and their percentage contributions.

5. Database survey

A search of the Cambridge Structural Database (CSD, Version 6.01, updated of November 2025; (Groom *et al.*, 2016) performed using Conquest (Bruno *et al.*, 2002) for the 2-amino-4-methylpyridin-1-ium cation yielded 62 entries corresponding to salt forms. A number of these salts are with substituted benzoic acids such as 2-hydroxybenzoic acid (CSD refcode DUTZOI) and 3-hydroxybenzoic acid (AGAQIK) (Khalib *et al.*, 2013), 2- and 4-chlorobenzoic acids (COZVAQ and COZVOE); 4-methylbenzoic acid (COZVIY) (Khalib *et al.*, 2014); and 4-nitrobenzoic acid (DUNCOF; Hemamalini & Fun, 2010*a*), as well as other related substituted benzoates.

Salts with aliphatic carboxylic acids have also been reported, including succinic acid (DICYEW; Seth *et al.*, 2018), fumaric acid (DUSPUD; Hemamalini & Fun, 2010*c*), trifluoroacetic acid (KUSVAW; Hemamalini & Fun, 2010*b*), sorbic acid (SUZXUH; Hemamalini & Fun, 2010*d*), oxalic acid (YIZDAQ; Hemalatha *et al.*, 2023) and tartaric acid (YOHHIO; Jovita *et al.*, 2014).

A separate search for the hippurate anion revealed eight structures in the CSD. These correspond to salts of hippuric acid with various active pharmaceutical ingredients (APIs) and biologically relevant bases, including imatinib (AJIPOC) (Jiang *et al.*, 2025); ciprofloxacin (OSUQEA; Chadha *et al.*, 2016); cytosine (CYTBGL01); Görbitz & Sagstuen, 2004) guanidine (BEMWOJ; Reena *et al.*, 2022) and acridine (XANSOY; Suganya *et al.*, 2021). These results indicate that, although salts of the individual components are well documented in the structural database, structures comprising both components in a single salt are comparatively uncommon. The available entries further underscore the conformational flexibility and supramolecular versatility of the hippurate anion, which consistently assembles into stable crystal architectures primarily via classical N—H···O and O—H···O hydrogen-bonding interactions.

6. Synthesis and crystallization

Hot methanol solutions (50 mL) of 2-amino-4-methylpyridine (1.08 g, 1.00 mmol) and hippuric acid (1.80 g, 1.00 mmol) were mixed and warmed over a heating magnetic stirrer hotplate for 6h. The reaction mixture was stirred at room temperature for 6 h to obtain a clear homogeneous solution. The resulting solution was filtered and allowed to evaporate slowly at room temperature. Colourless block-shaped crystals suitable for single-crystal X-ray diffraction were obtained after approximately 10 days.

7. Refinement

Crystal data, data collection and structure refinement details are summarized in Table 2. H atoms were positioned geometrically (C—H = 0.93–0.96 Å) and refined as riding with $U_{iso}(H) = 1.2U_{eq}(C)$.

Table 2
Experimental details.

Crystal data	
Chemical formula	$C_6H_9N_2^+·C_9H_8NO_3^-·2(H_2O)$
M_r	323.35
Crystal system, space group	Orthorhombic, *Pbca*
Temperature (K)	298
a, *b*, *c* (Å)	15.137 (3), 7.3028 (14), 30.583 (6)
V (Å^3)	3380.7 (11)
Z	8
Radiation type	Cu *Kα*
μ (mm^{-1})	0.81
Crystal size (mm)	0.35 × 0.24 × 0.22
Data collection	
Diffractometer	Bruker D8 Venture Diffractometer
Absorption correction	Multi-scan (*SADABS*; Krause *et al.*, 2015)
T_{min}, T_{max}	0.547, 0.753
No. of measured, independent and observed [$I > 2\sigma(I)$] reflections	24560, 3208, 2918
R_{int}	0.051
$(\sin\theta/\lambda)_{max}$ (Å^{-1})	0.610
Refinement	
$R[F^2 > 2\sigma(F^2)]$, $wR(F^2)$, *S*	0.053, 0.153, 1.09
No. of reflections	3208
No. of parameters	234
No. of restraints	8
H-atom treatment	H atoms treated by a mixture of independent and constrained refinement
$\Delta\rho_{max}$, $\Delta\rho_{min}$ (e Å^{-3})	0.20, −0.20

Computer programs: *APEX4*, *SAINT* and *XPREP* (Bruker, 2021), *SHELXT2014/5* (Sheldrick, 2015*a*), *SHELXL2014/3* (Sheldrick, 2015*b*), *ORTEP-3 for Windows* (Farrugia, 2012), *Mercury* (Macrae *et al.*, 2020) and *PLATON* (Spek, 2020).

Acknowledgements

The authors gratefully acknowledge SAIF, IIT Madras, for the SCXRD data collection.

References

Aakeröy, C. B. & Seddon, K. R. (1993). *Chem. Soc. Rev.* **22**, 397–407.
Bedeković, N., Stilinović, V. & Piteša, T. (2017). *Cryst. Growth Des.* **17**, 5732–5743.
Bis, J. A. & Zaworotko, M. J. (2005). *Cryst. Growth Des.* **5**, 1169–1179.
Bruker (2021). *APEX4*, *SAINT* and *XPREP*. Bruker AXS Inc., Madison, Wisconsin, USA.
Bruno, I. J., Cole, J. C., Edgington, P. R., Kessler, M., Macrae, C. F., McCabe, P., Pearson, J. & Taylor, R. (2002). *Acta Cryst.* B**58**, 389–397.
Budzikur, D., Kinzhybalo, V. & Ślepokura, K. (2022). *CrystEngComm* **24**, 4417–4429.
Chadha, R., Singh, P., Khullar, S. & Mandal, S. K. (2016). *Cryst. Growth Des.* **16**, 4960–4967.
Cruz-Cabeza, A. J. (2012). *CrystEngComm* **14**, 6362–6365.
Cruz-Cabeza, A. J., Lusi, M., Wheatcroft, H. P. & Bond, A. D. (2022). *Faraday Discuss.* **235**, 446–466.
Desiraju, G. R. (2002). *Acc. Chem. Res.* **35**, 565–573.
Farrugia, L. J. (2012). *J. Appl. Cryst.* **45**, 849–854.
Görbitz, C. H. & Sagstuen, E. (2004). *Acta Cryst.* E**60**, o1945–o1947.
Groom, C. R., Bruno, I. J., Lightfoot, M. P. & Ward, S. C. (2016). *Acta Cryst.* B**72**, 171–179.
Hemalatha, B., Suresh, S. & Poomani, K. (2023). *Chem. Data Collect.* 48, 101100.
Hemamalini, M. & Fun, H.-K. (2010*a*). *Acta Cryst.* E**66**, o335.
Hemamalini, M. & Fun, H.-K. (2010*b*). *Acta Cryst.* E**66**, o781–o782.

Hemamalini, M. & Fun, H.-K. (2010*c*). *Acta Cryst.* E**66**, o1962–o1963.
Hemamalini, M. & Fun, H.-K. (2010*d*). *Acta Cryst.* E**66**, o2397–o2398.
Jiang, Q., Ghosh, R. K., Valdivia-Berroeta, G. A., Walder, B. J. & Luo, L. (2025). *Cryst. Growth Des.* **25**, 1978–1991.
Jovita, J. V., Sathya, S., Usha, G., Vasanthi, R. & Ramanand, A. (2014). *Acta Cryst.* E**70**, o1036–o1037.
Khalib, N. C., Thanigaimani, K., Arshad, S. & Razak, I. A. (2013). *Acta Cryst.* E**69**, o1120.
Khalib, N. C., Thanigaimani, K., Arshad, S. & Razak, I. A. (2014). *J. Chem. Crystallogr.* **44**, 555–571.
Konovalova, I. S. & Reiss, G. J. (2025). *Crystals* **15**, 700.
Krause, L., Herbst-Irmer, R., Sheldrick, G. M. & Stalke, D. (2015). *J. Appl. Cryst.* **48**, 3–10.
Kvick, Å. & Noordik, J. (1977). *Acta Cryst.* B**33**, 2862–2866.
Laishram, R., Singh, A. R., Devi, S. S., Thomson, N., Chanu, W. P., Sieroń, L., Maniukiewicz, W. & Lonibala, R. (2025). *Polyhedron* **280**, 117682.
Li, W., Dong, H., Niu, K., Wang, H.-Y., Cheng, W., Song, H., Ying, A.-K., Zhai, X., Li, K., Yu, H., Guo, D.-S. & Wang, Y. (2024). *Talanta* **278**, 126480.
Macrae, C. F., Sovago, I., Cottrell, S. J., Galek, P. T. A., McCabe, P., Pidcock, E., Platings, M., Shields, G. P., Stevens, J. S., Towler, M. & Wood, P. A. (2020). *J. Appl. Cryst.* **53**, 226–235.
Reena, P., Joema, S. E., Gunasekaran, B., Sindhusha, S., Sabari Girisun, T. C. & Darling, D. A. (2022). *Opt. Mater.* **132**, 112749.
Seth, S. K., Bauzá, A. & Frontera, A. (2018). *New J. Chem.* **42**, 12134–12142.
Sheldrick, G. M. (2015*a*). *Acta Cryst.* A**71**, 3–8.
Sheldrick, G. M. (2015*b*). *Acta Cryst.* C**71**, 3–8.
Spek, A. L. (2020). *Acta Cryst.* E**76**, 1–11.
Suganya, S., Saravanan, K., Jaganathan, R. & Kumaradhas, P. (2021). *Acta Cryst.* C**77**, 790–799.
Turner, M., McKinnon, J., Wolff, S., Grimwood, D., Spackman, P., Jayatilaka, D. & Spackman, M. (2017). University of Western Australia.
Vetrivel, V., Balakrishnan, T. & Marimuthu, N. (2025). *Acta Cryst.* E**81**, 1189–1194.

supporting information

Acta Cryst. (2026). E**82**, 702-706 [https://doi.org/10.1107/S2056989026004846]

Synthesis and structure of 2-amino-4-methylpyridin-1-ium hippurate dihydrate

Vanitha Vetrivel, Nishandhini Marimuthu and Thangavelu Balakrishnan

Computing details

2-Amino-4-methylpyridin-1-ium 2-(phenylformamido)acetate dihydrate

Crystal data

$C_6H_9N_2^+ \cdot C_9H_8NO_3^- \cdot 2(H_2O)$
$M_r = 323.35$
Orthorhombic, *Pbca*
$a = 15.137$ (3) Å
$b = 7.3028$ (14) Å
$c = 30.583$ (6) Å
$V = 3380.7$ (11) Å^3
$Z = 8$
$F(000) = 1376$
$D_x = 1.271$ Mg m^{-3}
Cu $K\alpha$ radiation, $\lambda = 1.54178$ Å
Cell parameters from 7667 reflections
$\theta = 4.1$–$70.0°$
$\mu = 0.81$ mm^{-1}
$T = 298$ K
Block, colourless
0.35 × 0.24 × 0.22 mm

Data collection

Bruker D8 Venture Diffractometer
Radiation source: micro focus sealed tube
φ and ω scans
Absorption correction: multi-scan (SADABS; Krause *et al.*, 2015)
$T_{min} = 0.547$, $T_{max} = 0.753$
24560 measured reflections
3208 independent reflections
2918 reflections with $I > 2\sigma(I)$
$R_{int} = 0.051$
$\theta_{max} = 70.0°$, $\theta_{min} = 2.9°$
$h = -18 \rightarrow 18$
$k = -8 \rightarrow 8$
$l = -34 \rightarrow 37$

Refinement

Refinement on F^2
Least-squares matrix: full
$R[F^2 > 2\sigma(F^2)] = 0.053$
$wR(F^2) = 0.153$
$S = 1.09$
3208 reflections
234 parameters
8 restraints
Hydrogen site location: mixed
H atoms treated by a mixture of independent and constrained refinement
$w = 1/[\sigma^2(F_o^2) + (0.0923P)^2 + 0.350P]$ where $P = (F_o^2 + 2F_c^2)/3$
$(\Delta/\sigma)_{max} = 0.001$
$\Delta\rho_{max} = 0.20$ e Å^{-3}
$\Delta\rho_{min} = -0.19$ e Å^{-3}
Extinction correction: SHELXL2019/2 (Sheldrick 2015b), $Fc^* = kFc[1+0.001xFc^2\lambda^3/\sin(2\theta)]^{-1/4}$
Extinction coefficient: 0.0072 (6)

Special details

Geometry. All esds (except the esd in the dihedral angle between two l.s. planes) are estimated using the full covariance matrix. The cell esds are taken into account individually in the estimation of esds in distances, angles and torsion angles; correlations between esds in cell parameters are only used when they are defined by crystal symmetry. An approximate (isotropic) treatment of cell esds is used for estimating esds involving l.s. planes.

Fractional atomic coordinates and isotropic or equivalent isotropic displacement parameters (Å²)

	x	*y*	*z*	U_{iso}*/U_{eq}
C1	0.52405 (11)	0.6531 (2)	0.55085 (5)	0.0634 (4)
C2	0.57345 (12)	0.5010 (3)	0.56117 (6)	0.0820 (5)
H2	0.553559	0.420177	0.582510	0.098*
C3	0.65265 (14)	0.4676 (3)	0.53993 (7)	0.0976 (6)
H3	0.685875	0.364962	0.547277	0.117*
C4	0.68232 (13)	0.5843 (4)	0.50824 (6)	0.0949 (6)
H4	0.735675	0.561428	0.494186	0.114*
C5	0.63421 (17)	0.7325 (4)	0.49740 (7)	0.0992 (7)
H5	0.654065	0.811233	0.475605	0.119*
C6	0.55571 (15)	0.7679 (3)	0.51848 (7)	0.0886 (5)
H6	0.523277	0.871148	0.510788	0.106*
C7	0.43806 (12)	0.6994 (2)	0.57182 (5)	0.0653 (4)
C8	0.30803 (10)	0.5937 (2)	0.61047 (5)	0.0666 (4)
H8A	0.275980	0.478744	0.609411	0.080*
H8B	0.276331	0.680558	0.592319	0.080*
C9	0.30683 (10)	0.6635 (2)	0.65749 (5)	0.0614 (4)
C10	0.22844 (9)	0.12490 (18)	0.27751 (4)	0.0547 (3)
C11	0.24565 (10)	0.05872 (18)	0.32012 (4)	0.0588 (4)
H11	0.198861	0.022428	0.337826	0.071*
C12	0.32969 (10)	0.0475 (2)	0.33553 (5)	0.0636 (4)
C13	0.40030 (11)	0.1037 (3)	0.30865 (6)	0.0742 (4)
H13	0.458206	0.099824	0.318772	0.089*
C14	0.38185 (11)	0.1635 (3)	0.26776 (6)	0.0743 (5)
H14	0.427978	0.199248	0.249575	0.089*
C15	0.34820 (14)	−0.0249 (3)	0.38085 (6)	0.0892 (6)
H15A	0.365066	0.074466	0.399619	0.134*
H15B	0.395280	−0.112843	0.379533	0.134*
H15C	0.296011	−0.082495	0.392225	0.134*
N1	0.39430 (9)	0.56514 (17)	0.59169 (4)	0.0621 (3)
H1	0.4169 (11)	0.458 (2)	0.5917 (6)	0.074*
N2	0.29813 (8)	0.17252 (17)	0.25277 (4)	0.0623 (3)
H2A	0.2858 (11)	0.212 (2)	0.2254 (5)	0.075*
N3	0.14821 (9)	0.1412 (2)	0.26100 (4)	0.0677 (4)
O1	0.40736 (11)	0.85655 (16)	0.56980 (5)	0.0929 (4)
O2	0.37639 (8)	0.67686 (18)	0.67853 (4)	0.0767 (4)
O3	0.23079 (7)	0.70195 (18)	0.67150 (4)	0.0753 (4)
H3A	0.1393 (13)	0.192 (3)	0.2350 (5)	0.090*
H3B	0.1007 (11)	0.123 (3)	0.2784 (6)	0.090*
O4	0.58180 (8)	0.82361 (16)	0.37897 (4)	0.0752 (4)
H4A	0.6302 (14)	0.835 (3)	0.3632 (7)	0.113*
H4B	0.5816 (16)	0.926 (3)	0.3936 (8)	0.113*
O5	0.48776 (8)	0.5845 (2)	0.32339 (4)	0.0810 (4)
H5A	0.5105 (18)	0.668 (3)	0.3383 (9)	0.122*
H5B	0.5277 (16)	0.498 (3)	0.3257 (9)	0.122*

Atomic displacement parameters (Å²)

	U^{11}	U^{22}	U^{33}	U^{12}	U^{13}	U^{23}
C1	0.0790 (9)	0.0570 (8)	0.0541 (7)	−0.0026 (6)	−0.0060 (6)	−0.0066 (6)
C2	0.0823 (11)	0.0888 (12)	0.0747 (10)	0.0142 (9)	0.0078 (8)	0.0155 (9)
C3	0.0814 (11)	0.1203 (17)	0.0911 (13)	0.0221 (11)	0.0085 (10)	0.0122 (12)
C4	0.0799 (11)	0.1351 (19)	0.0696 (10)	−0.0122 (12)	0.0047 (8)	−0.0119 (11)
C5	0.1157 (16)	0.1059 (16)	0.0761 (11)	−0.0271 (14)	0.0145 (11)	0.0030 (11)
C6	0.1159 (15)	0.0685 (10)	0.0816 (11)	−0.0032 (10)	0.0058 (10)	0.0065 (9)
C7	0.0876 (10)	0.0498 (8)	0.0586 (8)	0.0082 (7)	−0.0076 (7)	−0.0093 (6)
C8	0.0699 (9)	0.0698 (9)	0.0602 (8)	0.0084 (7)	−0.0062 (6)	−0.0154 (7)
C9	0.0645 (8)	0.0597 (8)	0.0600 (8)	0.0067 (6)	−0.0044 (6)	−0.0096 (6)
C10	0.0623 (8)	0.0475 (7)	0.0544 (7)	0.0030 (5)	0.0057 (5)	−0.0001 (5)
C11	0.0690 (8)	0.0530 (7)	0.0544 (7)	0.0020 (6)	0.0067 (6)	0.0014 (5)
C12	0.0738 (9)	0.0575 (8)	0.0595 (8)	0.0052 (6)	−0.0026 (6)	−0.0039 (6)
C13	0.0642 (8)	0.0820 (11)	0.0765 (10)	0.0032 (7)	−0.0022 (7)	0.0011 (8)
C14	0.0621 (8)	0.0838 (11)	0.0770 (10)	−0.0003 (7)	0.0113 (7)	0.0041 (8)
C15	0.0932 (12)	0.1075 (14)	0.0669 (10)	0.0085 (11)	−0.0128 (9)	0.0097 (9)
N1	0.0744 (8)	0.0522 (6)	0.0596 (7)	0.0106 (5)	−0.0007 (5)	−0.0081 (5)
N2	0.0652 (7)	0.0642 (7)	0.0574 (7)	0.0041 (5)	0.0092 (5)	0.0053 (5)
N3	0.0623 (7)	0.0802 (9)	0.0607 (7)	0.0035 (6)	0.0047 (5)	0.0136 (6)
O1	0.1266 (11)	0.0521 (7)	0.1000 (9)	0.0204 (6)	0.0054 (8)	−0.0046 (6)
O2	0.0679 (7)	0.0963 (8)	0.0658 (6)	0.0137 (5)	−0.0098 (5)	−0.0226 (5)
O3	0.0647 (7)	0.0951 (8)	0.0660 (6)	0.0101 (5)	−0.0031 (5)	−0.0206 (6)
O4	0.0689 (7)	0.0668 (7)	0.0900 (8)	−0.0026 (5)	0.0090 (6)	−0.0152 (6)
O5	0.0726 (7)	0.0918 (9)	0.0787 (8)	0.0119 (6)	−0.0210 (6)	−0.0044 (6)

Geometric parameters (Å, º)

C1—C2	1.376 (2)	C10—N2	1.3439 (18)
C1—C6	1.383 (3)	C10—C11	1.4142 (19)
C1—C7	1.490 (2)	C11—C12	1.359 (2)
C2—C3	1.385 (3)	C11—H11	0.9300
C2—H2	0.9300	C12—C13	1.409 (2)
C3—C4	1.367 (3)	C12—C15	1.510 (2)
C3—H3	0.9300	C13—C14	1.354 (3)
C4—C5	1.346 (3)	C13—H13	0.9300
C4—H4	0.9300	C14—N2	1.349 (2)
C5—C6	1.376 (3)	C14—H14	0.9300
C5—H5	0.9300	C15—H15A	0.9600
C6—H6	0.9300	C15—H15B	0.9600
C7—O1	1.2394 (19)	C15—H15C	0.9600
C7—N1	1.330 (2)	N1—H1	0.851 (14)
C8—N1	1.442 (2)	N2—H2A	0.904 (15)
C8—C9	1.526 (2)	N3—H3A	0.888 (15)
C8—H8A	0.9700	N3—H3B	0.903 (15)
C8—H8B	0.9700	O4—H4A	0.881 (17)
C9—O2	1.2377 (18)	O4—H4B	0.872 (17)

C9—O3	1.2598 (19)	O5—H5A	0.834 (17)
C10—N3	1.3205 (19)	O5—H5B	0.879 (17)
C2—C1—C6	117.73 (17)	N3—C10—C11	123.54 (13)
C2—C1—C7	124.01 (14)	N2—C10—C11	117.56 (13)
C6—C1—C7	118.25 (15)	C12—C11—C10	120.83 (13)
C1—C2—C3	120.33 (18)	C12—C11—H11	119.6
C1—C2—H2	119.8	C10—C11—H11	119.6
C3—C2—H2	119.8	C11—C12—C13	119.33 (14)
C4—C3—C2	120.5 (2)	C11—C12—C15	120.87 (15)
C4—C3—H3	119.8	C13—C12—C15	119.79 (16)
C2—C3—H3	119.8	C14—C13—C12	118.45 (16)
C5—C4—C3	119.9 (2)	C14—C13—H13	120.8
C5—C4—H4	120.0	C12—C13—H13	120.8
C3—C4—H4	120.0	N2—C14—C13	121.56 (15)
C4—C5—C6	120.2 (2)	N2—C14—H14	119.2
C4—C5—H5	119.9	C13—C14—H14	119.2
C6—C5—H5	119.9	C12—C15—H15A	109.5
C5—C6—C1	121.4 (2)	C12—C15—H15B	109.5
C5—C6—H6	119.3	H15A—C15—H15B	109.5
C1—C6—H6	119.3	C12—C15—H15C	109.5
O1—C7—N1	121.22 (17)	H15A—C15—H15C	109.5
O1—C7—C1	121.09 (16)	H15B—C15—H15C	109.5
N1—C7—C1	117.66 (13)	C7—N1—C8	121.76 (13)
N1—C8—C9	115.75 (12)	C7—N1—H1	118.4 (13)
N1—C8—H8A	108.3	C8—N1—H1	119.7 (13)
C9—C8—H8A	108.3	C10—N2—C14	122.22 (13)
N1—C8—H8B	108.3	C10—N2—H2A	116.2 (11)
C9—C8—H8B	108.3	C14—N2—H2A	121.6 (11)
H8A—C8—H8B	107.4	C10—N3—H3A	121.3 (13)
O2—C9—O3	125.66 (13)	C10—N3—H3B	119.6 (13)
O2—C9—C8	120.40 (13)	H3A—N3—H3B	117.8 (19)
O3—C9—C8	113.94 (13)	H4A—O4—H4B	102 (2)
N3—C10—N2	118.90 (13)	H5A—O5—H5B	101 (3)
C6—C1—C2—C3	0.9 (3)	N3—C10—C11—C12	−179.07 (14)
C7—C1—C2—C3	179.70 (18)	N2—C10—C11—C12	1.2 (2)
C1—C2—C3—C4	−0.6 (3)	C10—C11—C12—C13	0.4 (2)
C2—C3—C4—C5	−0.3 (3)	C10—C11—C12—C15	−179.38 (15)
C3—C4—C5—C6	0.7 (3)	C11—C12—C13—C14	−1.5 (2)
C4—C5—C6—C1	−0.4 (3)	C15—C12—C13—C14	178.29 (17)
C2—C1—C6—C5	−0.5 (3)	C12—C13—C14—N2	1.0 (3)
C7—C1—C6—C5	−179.33 (17)	O1—C7—N1—C8	2.2 (2)
C2—C1—C7—O1	161.68 (17)	C1—C7—N1—C8	−175.96 (12)
C6—C1—C7—O1	−19.5 (2)	C9—C8—N1—C7	−87.11 (18)
C2—C1—C7—N1	−20.2 (2)	N3—C10—N2—C14	178.47 (15)
C6—C1—C7—N1	158.64 (15)	C11—C10—N2—C14	−1.8 (2)
N1—C8—C9—O2	−6.4 (2)	C13—C14—N2—C10	0.7 (3)

N1—C8—C9—O3	174.15 (14)

Hydrogen-bond geometry (Å, º)

D—H···*A*	*D*—H	H···*A*	*D*···*A*	*D*—H···*A*
O5—H5*A*···O4	0.83 (2)	2.00 (2)	2.8225 (18)	167 (3)
N1—H1···O4^{i}	0.85 (1)	2.25 (2)	2.9992 (18)	148 (2)
N2—H2*A*···O3^{ii}	0.90 (2)	1.78 (2)	2.6850 (17)	176 (2)
N3—H3*A*···O2^{ii}	0.89 (2)	1.99 (2)	2.8751 (17)	175 (2)
N3—H3*B*···O5^{iii}	0.90 (2)	1.94 (2)	2.8368 (18)	171 (2)
O4—H4*A*···O3^{iv}	0.88 (2)	1.88 (2)	2.7392 (17)	166 (2)
O4—H4*B*···O1^{v}	0.87 (2)	1.95 (2)	2.8173 (18)	173 (2)
O5—H5*B*···O2^{i}	0.88 (2)	1.94 (2)	2.8061 (18)	170 (3)

Symmetry codes: (i) −*x*+1, −*y*+1, −*z*+1; (ii) −*x*+1/2, −*y*+1, *z*−1/2; (iii) −*x*+1/2, *y*−1/2, *z*; (iv) *x*+1/2, −*y*+3/2, −*z*+1; (v) −*x*+1, −*y*+2, −*z*+1.